NASA Contractor Report 174740

Thermal-Mechanical Fatigue Crack Growth in Inconel X-750

Normand Marchand and Regis M. Pelloux

Massachusetts Institute of Technology
Cambridge, Massachusetts

October 1984

Prepared for

NATIONAL AERONAUTICS AND SPACE ADMINISTRATION
Lewis Research Center
Under Grant NAG 3-280

Thermal-Mechanical Fatigue Crack Growth in Inconel X-750

by

N. Marchand and R. Pelloux
Massachusetts Institute of Technology

Thermal-mechanical fatigue (TMF)crack growth experiments were conducted on notched inconel x-750 specimens. Temperature was cycled between 300°C and 650°C and stress controlled mechanical cycling was imposed in-phase (maximum stress at maximum temperature) and out-of-phase (minimum stress at maximum temperature) with the thermal cycle. Three major contributions are identified with this paper. First, a technique for applying potential drop measurements to TMF experiments was developed. This technique required automated means of sorting out thermal resistivity changes associated with the material, and specimen resistance changes caused by crack growth and permitted real-time, cycle-by-cycle monitoring of TMF crack growth. Second, out-of-phase cycling was observed to be more damaging than in-phase cycling, a behavior not generally observed in Ni-based superalloys. Either the employment of stress controlled experiments or the rather low maximum temperature used may have been factors here. Finally, the crack growth data correlated very well with ΔK, provided a correction to ΔK was imposed to account for crack closure.

THERMAL-MECHANICAL FATIGUE CRACK GROWTH IN INCONEL X-750

Norman Marchand* and Regis M. Pelloux**

*Research Assistant, Department of Materials Science and Engineering, Massachusetts Institute of Technology, Cambridge, MA 02139, USA

**Professor, Department of Materials Science and Engineering, Massachusetts Institute of Technology, Cambridge, MA 02139, USA

ABSTRACT

Thermal-mechanical fatigue crack growth (TMFCG) was studied in a γ-γ' nickel-base superalloy Inconel X-750 under controlled load amplitude in the temperature range from 300 to 650°C. In-phase (T_{max} at σ_{max}), out-of-phase (T_{min} at σ_{max}) and isothermal tests at 650°C were performed on single-edge notch bars under fully reversed cyclic conditions.

A DC electrical potential method was used to measure crack length. The electrical potential response obtained for each cycle of a given wave form and R value yields information on crack closure and crack extension per cycle. The macroscopic crack growth rates are reported as a function of ΔK and the relative magnitude of the TMFCG are discussed in the light of the potential drop information and of the fractographic observations.

INTRODUCTION

Many fatigue problems in high temperature machinery such as gas turbine components involve thermal as well as mechanical loadings. By thermal loading it is meant that the material is subjected to cyclic temperature simultaneously with cyclic stress or strain. Analysis of the local stresses and strains versus temperature and time become very complex, consequently gross simplifications are introduced to analyse and predict the fatigue damage. These simplifications usually involve the use of isothermal data and life predictions techniques are based upon isothermal testing. In fact, the study of fatigue has generally bypassed real thermal fatigue loading partly because isothermal tests are relatively simple to perform, but also because it has often been felt that such tests carried out at the maximum service temperature would give worst case results. However, several studies which have compared fatigue resistance under thermal cycling conditions with that in isothermal tests have shown that in many cases, the latter, rather than giving a worst case situation, can seriously overestimate the real fatigue life [1-15].

The influence of temperature on low cycle fatigue (LCF) lives is well documented [16-19] but the mechanisms by which temperature influences the fatigue process are not well understood. Low cycle fatigue is generally acknowledged to be directly related to material ductility; however, as ductility increases with temperature, low cycle fatigue life normally decreases. Creep and environmental effects are known to influence the LCF behavior, but the relative contributions of these two factors are not easily differentiated [17-19, 20].

The subject of thermal fatigue which involves combined temperature and stress-strain cycling, is less well understood than isothermal elevated temperature fatigue and only limited data have been gathered on crack growth during thermal-mechanical fatigue (TMF) under conditions of small plastic strain [2, 5-7, 9, 13-14].

The data obtained from thermal-mechanical testing for conventionally cast Co- and Ni-based superalloys, and for directionally solidified Ni-based alloy [5-7, 9, 13] have shown faster crack growth rates than for the equivalent isothermal conditions at T_{max}. Furthermore, crack growth rates under out-of-phase cycling (T_{min} at σ_{max}) were found to be faster than under in-phase cycling (T_{max} at σ_{max}). For a 12 Cr-Mo-V-W steel thermal-mechanically cycle between 300 and 600°C, very little difference in growth rates for TMF and isothermal tests were found [21], whereas, an inverse behavior was observed on a 304 SS [15]; that is, faster crack growth rates under in-phase cycling than under out-of-phase cycling.

From the TMF crack growth data available in the open literature, it can be seen that there is no generalization to be made concerning the severity of damage associated with in-phase and out-of-phase cycling, and that there is no hard and fast rule for relating TMF data to isothermal testing.

In order to obtain a better understanding of the TMFCG behavior, a research program was established with a two-fold objective. First, to assess a sound, fundamental mechanistic understanding of TMF of typical nickel-base superalloys. Second, to assess the suitability of various parameters for correlating high temperature TMFCG rates used for adequate fatigue life predictions of engine components.

EXPERIMENTAL PROCEDURE

Materials and Specimen

The material used in this investigation was a standard chemistry Inconel X-750, a corrosion and oxidation resistant material with good tensile and creep properties at elevated temperatures. The chemical composition, the heat treatment of the as-received annealed material, and the tensile properties at high and room temperature are given in Table 1. The grain size is about 0.12mm. Single edge notch tensile

bar specimens were used in this investigation. The test specimens have a rectangular cross-section of 11.7 x 4.4 mm^2 and a starter notch approximately 1 mm deep, which is cut by electro-discharge machining. The specimens were pre-cracked in fatigue at 10 Hz at room temperature under a ΔK of about 10-15 MPa $\sqrt{m}$. All the ΔK's were calculated with the expression derived by Harris [22].

$$\Delta K = \Delta\sigma \sqrt{\pi a} \frac{5}{[20 - 13(\frac{a}{w}) - 7(\frac{a}{w})^2]^{\frac{1}{2}}} \quad (1)$$

This formula which was derived for an edge crack in a SEN plate with no bending is suitable for the testing system.

Table 1

(a) Chemical Composition (wt. pct.)

Ni	Cr	Fe	Ti	Al	Nb	Mn	Si	C	Co
72	15.5	7	2.5	0.7	1	0.5	0.2	0.04	1.0

(b) Heat Treatment

Temperature (°C)	Time (hr)	Quench
1150	2	air cool
850	24	air cool
700	20	air cool

(c) Tensile Properties

Temperature (°C)	σ_y(MPa)	σ_{UTS}(MPa)	ϵ_p(Pct)
24	610	1000	30
300	616	1000	32
650	550	820	7

Apparatus and Test Conditions

The apparatus used in this study was a computer-controlled thermal fatigue testing system which consisted of a closed-loop servo-controlled, electro-hydraulic tension-compression fatigue machine, a high frequency oscillator for induction heating, an air compressor for cooling, a mini-computer, etc. Figure 1 shows the control block diagram of this system.

The system is capable of testing specimens of different sizes and configurations (SEN, CT, hollow tube, etc.) up to loads of 25,000 lbs. The specimen alignment is insured by the use of a Wood's metal pot

which prevents a bending moment in the specimen. Because a DC potential drop technique is used to monitor crack growth, the lower grip is electrically insulated from the system by means of a ceramic coating. The ends of the grips are water cooled by means of copper coils.

Temperature was measured with 0.2 mm diameter chromel-alumel thermocouples which were spot welded along the gauge length. By computer controlling, the temperature in the gauge length was maintained within 5°C of the desired temperature for both axial and transverse directions over the entire period of the test.

Temperature and stress were computer controlled with the output of the thermocouple so that they were in-phase or out-of-phase for the same triangular wave shape. Therefore, specimens were in tension at low temperature and in compression at high temperature under the out-of-phase cycling, and vice versa under the in-phase fatigue. The temperature range in these tests was 300 to 650°C. The tests were carried out at a frequency of 0.0056 Hz (1/3 cpm) and were run at a R ratio ($\sigma_{min}/\sigma_{max}$) of -1 or 0.05. Isothermal fatigue tests were also conducted under the same frequency at T_{max} for comparison with the results of TMFCG tests. All the tests were carried out in air. Table 2 summarizes the experimental conditions. At least two tests at each condition were performed to insure repeatability of the results.

There have been few attempts to measure crack length in the TMF cycling using the potential drop technique [2]. The method has proved to be satisfactory in isothermal conditions and can be used for TMF testing provided that the electrical noise is adequately filtered and the calibration curve is properly corrected to take into account changes of potential with temperature. This was achieved by using a 450 KHz filter and a high accuracy digital voltmeter programmed to convert the analog signal average over 10 power line cycles (PLC). In this mode, 1 PLC is used for the run-up time with the A/D conversion repeated ten times. The resulting ten readings are then averaged and the answer becomes a single reading.

This system, as opposed to the optical measurement and compliance methods, has the capability of monitoring the crack extension during a single cycle, whereas the previous methods are limited for growth measurement to no more than one cycle. Therefore, detailed analysis of the crack growth process can be performed and this is particularly important in trying to determine the mechanisms involved with TMFCG or with the kinetics of short crack growth.

Table 2

Experimental Conditions

Frequency (Hz)	Temperature (°C)	R-Ratio
0.1	25	0.05
0.0056	650	0.05
0.0056	650	-1
0.0056	300-650 (in-phase)	0.05
0.0056	300-650 (in-phase)	-1
0.0056	650-300 (out-of-phase)	-1

Results and Discussion

Figures 2 and 3 show the variation of the potential with simultaneous change of the net stress and temperature for in-phase and out-of-phase cycling at low and high ΔK. In these figures, the potential change with stress and temperature $V(T,\sigma)$ and with temperature only $V(T)$ are plotted. The mechanical driving force $V(\sigma)$ which is the difference between $V(T,\sigma)$ and $V(T)$ are also plotted. In order to assess crack growth, the peak potential of each cycle was recorded and plots of the voltage versus the number of cycle (N) were obtained. Using an experimental calibration curve, the crack lengths versus N were derived. The crack growth rates were calculated using a seven-point incremental polynomial method. Figure 4 shows the results as a function of ΔK ($R = 0.05$) and K_{max} ($R = -1$).

First, it can be seen that the crack growth rates are higher for TMF cycling than for the equivalent isothermal condition (650°C) which is in agreement with the results obtained on other nickel-base alloys [5-7, 9, 13]. Secondly, it is observed (Figure 4) that the crack growth rates are higher for $R = -1$ than for $R = 0.05$ which indicates that compressive stresses play an important role in the mechanics of TMFCG. Comparison between out-of-phase and in-phase at $R = -1$ shows that out-of-phase cycling is more damaging than in-phase cycling at high ΔK, whereas at low ΔK, the crack growth rates are the same. The explanation for this behavior can be found in Figures 2 and 3. At low ΔK the potential curves $V(\sigma)$ for out-pf-phase and in-phase are similar which indicates that the mechanical driving force for cracking are similar and identical crack growth rates are therefore expected. As ΔK increases, however, the $V(\sigma)$ potential curves for both in-phase and out-of-phase cycling display characteristic features (Figure 3). The in-phase $V(\sigma)$ curve shows a smooth increase with σ_{net} up to the maximum followed by a sharp increase at σ_{max}. The potential then remains stable as σ_{net} starts to decrease and sharply falls as σ_{net} approaches zero. In the compression regime the potential smoothly decreases, reaches a minimum at σ_{min}, and finally increases as the stress increases again. On the other hand, the out-of-phase $V(\sigma)$ potential shows (at the same ΔK) a smooth increase with σ_{net} with a peak value at σ_{max}. The potential then decreases down to a minimum value and finally increases again with σ_{net}. The most

important feature of these signals is the crossover point (denoted A) for which $V(\sigma) = 0$. The crossover point represents the stress to apply to the specimen for the potential to equal V(T). Because V(T) is measured at $\sigma = 0$ for the entire thermal cycle, the expected stress to apply is $\sigma = 0$. However, if the potential field near the crack tip is disturbed either by a non-zero residual stress-strain field or by geometrical events such as blunting, closure, etc., the $V(T, \sigma = 0)$ potential might not necessarily equal V(T) and a non-zero stress is required to cancel out the contribution of this phenomena. For the out-of-phase potential, the crossover occurs at a negative stress ($\sigma = -75$ MPa at $\Delta K = 50$ MP a $\sqrt{m}$), whereas, it always occurs at zero stress for the in-phase potential. By first assuming that the crossover point occurs near an effective closure stress (σ_{cl}) it follows that the effective stress intensity factor (ΔK_{eff}) for crack growth will be higher for out-of-phase than for in-phase cycling (σ_{cl} is negative). If we plot the crack growth rates as a function of ΔK_{eff}, we find that both in-phase and out-of-phase crack growth rates overlap (Figure 5).

It is important to note that the absolute amplitude of the $V(\sigma)$ signal (see Figure 3) in the compressive regime of the cycle, is much higher for out-of-phase than for in-phase cycling which indicates that the crack surfaces are in contact on a much larger scale than under in-phase cycling. This was confirmed by fractographic observation which shows that out-of-phase cycling leads to transgranular cracking with considerable mating, whereas, in-phase cycling leads to intergranular fracture with little evidence of mating. The higher crack growth rates at $R = -1$ than $R = 0.05$ and the fractographic observations lead to the conclusion that although there should be no cracking at the maximum temperature because of the compressive stress, some form of severe damage is taking place under compressive strain. Also, the surface oxide film formed at high temperature will rupture at low temperature, under maximum tensile stress. This leads to a resharpening of the crack tip with each cycle and results in an increase in growth rate.

The rationale for the negative closure stress in out-of-phase cycling can be found by assuming that the residual stress field at the crack tip is of tensile nature at zero applied stress and that a negative stress has to be applied in order to cancel it and to close the crack. This negative σ_{cl} also represents the effective contribution to cracking of the damage taking place during the compression part of the cycle.

The difference in growth rates between the isothermal test (650°C) and the TMF tests were also explained by looking at their respective $V(\sigma)$ potential curves at low and high ΔK. At low ΔK no significant differences were observed between $V(\sigma)$ potential curves. At higher ΔK, however, the isothermal $V(\sigma)$ potential has shown a crossover point taking place at a positive stress. This has the effect of reducing the effective driving force for cracking. By taking into account this

σ_{cl} in tne computation of ΔK, one finds that the crack growth rates in terms of ΔK_{eff} for both isothermal and TMF tests are similar (Figure 5). The positive closure stress observed was attributed to the build-up of oxides in the wake of the crack. This is supported by fractographic observation which shows greater oxidation for isothermal testing than for TMF testing.

CONCLUSIONS

Faster crack growth rates were measured in Inconel X-750 cycled between 360 and 650°C under out-of-phase conditions than under in-phase cycling at R = -1 or R = 0.05. This behavior was rationalized by introducing the concept of an effective closure stress which was defined as the applied stress at the crossover point of the $V(\sigma)$ potential curve. σ_{cl} should represent the effective contribution to cracking of the damage taking place during the compressive part of the cycle. Correlation between TMFCG rates and ΔK appear to be valid provided elastic conditions prevailed in the bulk. Correction to the applied stress can be introduced in order to take into account damage occurring in the compressive part of the last cycle. Further work is needed to assess the suitability of ΔK to more realistic conditions involving TMFCG under cyclic plastic strains.

REFERENCES

1. Sheffler, K. D., Vacuum Thermal-Mechanical Fatigue Behavior of Two Iron-Base Alloys, ASTM STP 612, 1976, 214-226.

2. Skelton, R. P., Environmental Crack Growth in 1/2Cr-Mo-V Steel During Isothermal High Strain Fatigue and Temperature Cycling, Mat. Sci. Eng., Vol. 2, 1978, 287-298.

3. Fujino, N. and Tarai, S., Effect of Thermal Cycle on Low Cycle Fatigue Life of Steels and Grain Boundary Sliding Characteristics, ICM 3, Vol. 2, 1979, 49-58.

4. Kuwabara, K. and Nitta, A., Thermal-Mechanical Low Cycle Fatigue Under Creep-Fatigue Interaction in Type 304 Stainless Steel, ICM 3, Vol. 2, 1979, 69-78.

5. Rau, C. A., Gemma, A. E., Leverant, G. R., Thermal-Mechanical Fatigue Crack Propagation in Nickel and Cobalt Base Superalloys Under Various Strain-Temperature Cycles, ASTM STP 520, 1973, 166-178.

6. Gemma, A. E., Langer, B. S. and Leverant, G. R., Thermal-Mechanical Fatigue Crack Propagation in Anisotropic Nickel-Base Superalloys, ASTM STP 612, 1976, 199-213.

7. Gemma, A. E., Ashland, F. X. and Masci, R. M., The Effects of Stress Dwells and Varying Mean Strain on Crack Growth During Thermal Mechanical Fatigue, J. Test. Eval., Vol. 9, No. 4, 1981, 209-215.

8. Troshchenko, V. T. and Zaslotskaya, L. A., Fatigue Strength of Superalloys Subjected to Combined Mechanical and Thermal Loading, ICM 3, Vol. 2, 1979, 3-12.

9. Meyers, G. J., Fracture Mechanics Criteria for Turbine Engines and Hot Section Components, NASA CR-167896, 1982.

10. Jaske, C. E., Thermal-Mechanical Low Cycle Fatigue of AISI 1010 Steel, ASTM STP 612, 1976, 170-198.

11. Westwood, H. J. and Moles, M. D., Creep-Fatigue Problems in Electricity Generation Plants, Can. Met. Quart., Vol. 18, 1979, 215-230.

12. Bhongbhobhat, S., The Effect of Simultaneously Alternating Temperature and Hold Time in the Low Cycle Fatigue Behavior of Steels, Low Cycle Fatigue Strength and Elasto-Plastic Behavior of Materials, eds. Rie, K. T. and Harbach, E., DVM, 1979, 73-82.

13. Leverant, G. R., Strongman, T. E., and Langer, B. S., Parameters Controlling the Thermal Fatigue Properties of Conventional Cast and Directionally-Solidified Turbine Alloys, Superalloys: Metallurgy and Manufactures, ed., Kear, B. H., Muzuka, D. R., Tien, J. K., and Wlodek, S. T., Claxtors Pub., 1976, 285-295.

14. Okazaki, M. and Koizumi, T., Crack Propagation During Low Cycle Thermal-Mechanical and Isothermal Fatigue at Elevated Temperatures, Met. Trans., Vol. 14A, 1983, 1641-1648.

15. Kuwabara, K., Nitta, A., and Kitamura, T., Thermal-Mechanical Fatigue Life Prediction in High Temperature Component Materials for Power Plants, Conf. on Advances in Life Prediction Methods, ASME-MPC, Albany, N. Y., 1983, 131-141.

16. Wareing, J., Mechanisms of High Temperature Fatigue and Creep-Fatigue Failure in Engineering Materials, Fatigue at High Temperature, ed. Skelton, R. P., Applied Sci. Pub., 1983, 135-185.

17. Lloyd, G. J., High Temperature Fatigue and Creep-Fatigue Crack Propagation: Mechanics, Mechanisms and Observed Behavior in Structural Materials, Fatigue at High Temperature, ed. Skelton, R. P., Applied Sci. Pub., 1983, 187-258.

18. Coffin, L. F., Damage Processes in Time Dependent Fatigue - A Review, Creep-Fatigue-Environment Interactions, eds. Pelloux, R. M. and Stoloff, N. S., AIME, 1980, 1-23.

19. Mills, W. J. and James, L. A., Effect of Temperature on the Fatigue Crack Propagation Behavior of Inconel X-750, Fat. Eng. Mat. Struct., Vol. 3, 1980, 159-175.

20. Skelton, R. P., The Growth of Short Cracks During High Strain Fatigue and Thermal Cycling, ASTM STP 770, 1982, 337-381.

21. Koizumi, T. and Okazaki, M., Crack Growth and Prediction of Endurance in Thermal-Mechanical Fatigue of 12 Cr-Mo-V-W Steel, Fat. Eng. Mat. Struct., Vol. 1, 1979, 509-520.

22. Harris, D. O., Stress Intensity Factors for Hollow Circumferentially Notched Round Bars, J. Basic Eng., Vol. 89,1967, 49-54.

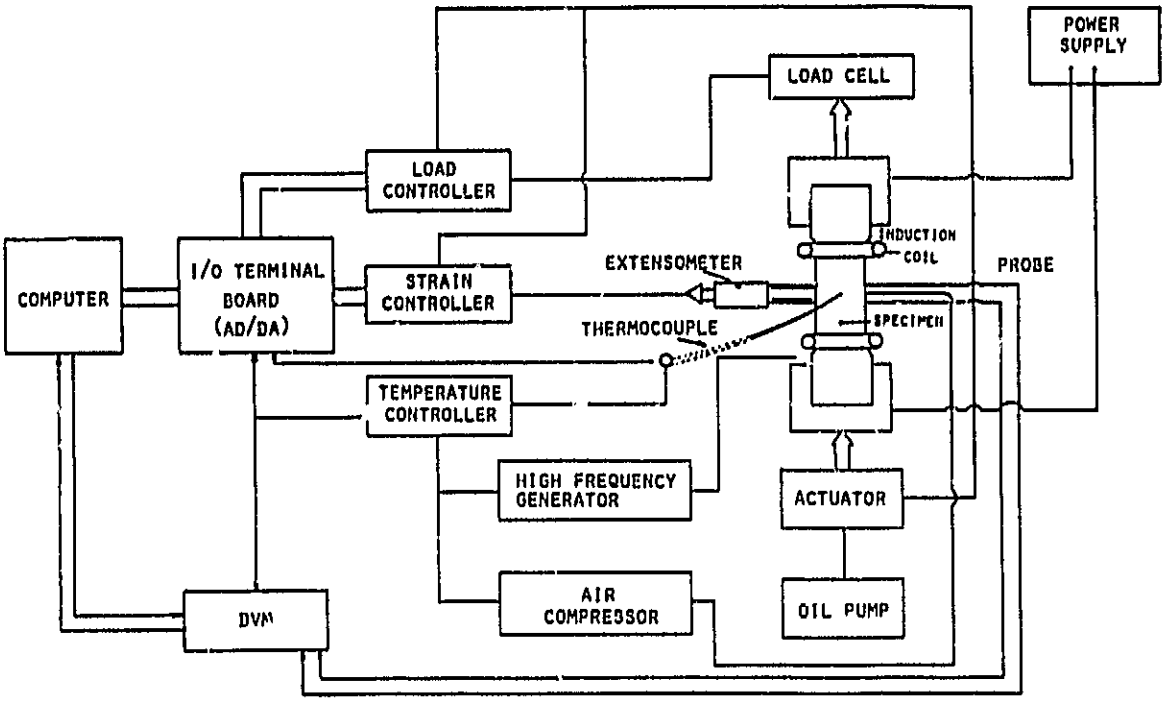

Figure 1 Diagram showing the control system of apparatus used for TMFCG tests.

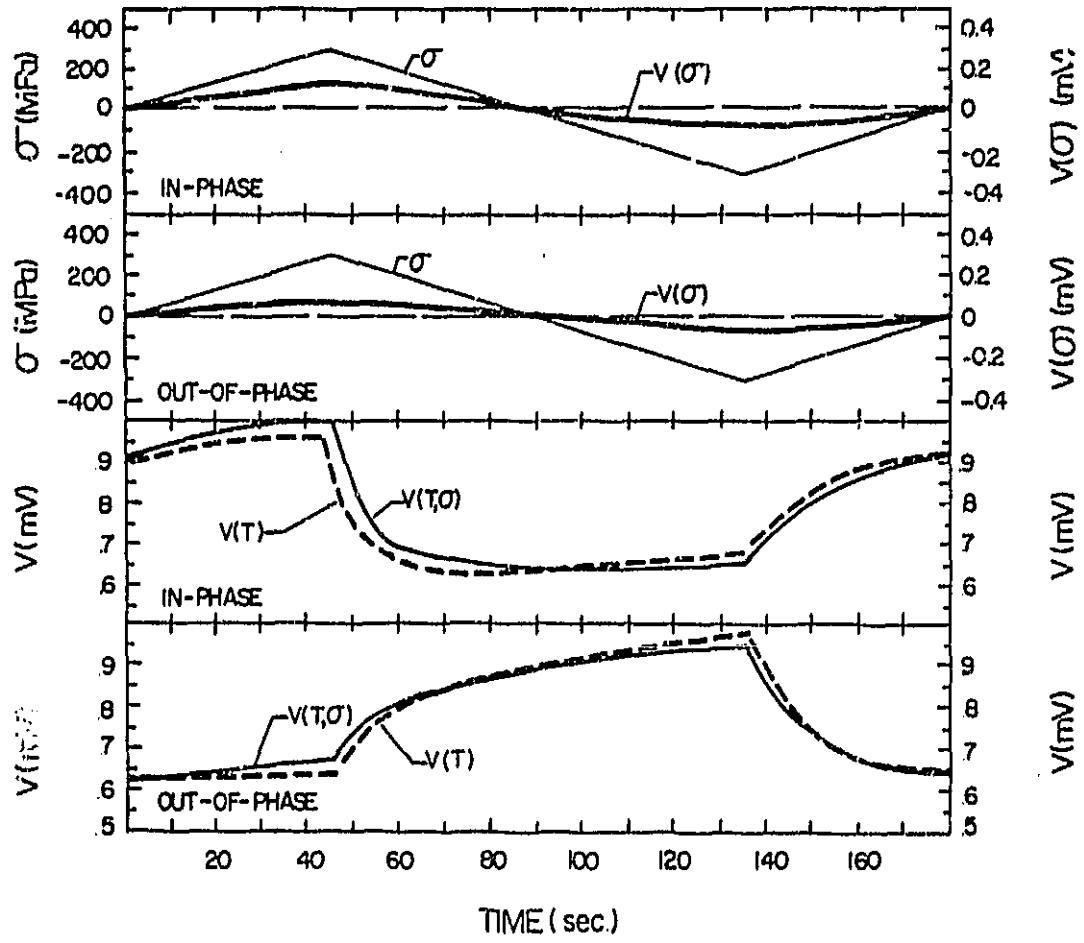

Figure 2 Potential curves $V(T, \sigma)$, $V(T)$ and $V(\sigma)$ for TMFCG of Inconel X-750. $\Delta K = 25$ MPa $\sqrt{m}$

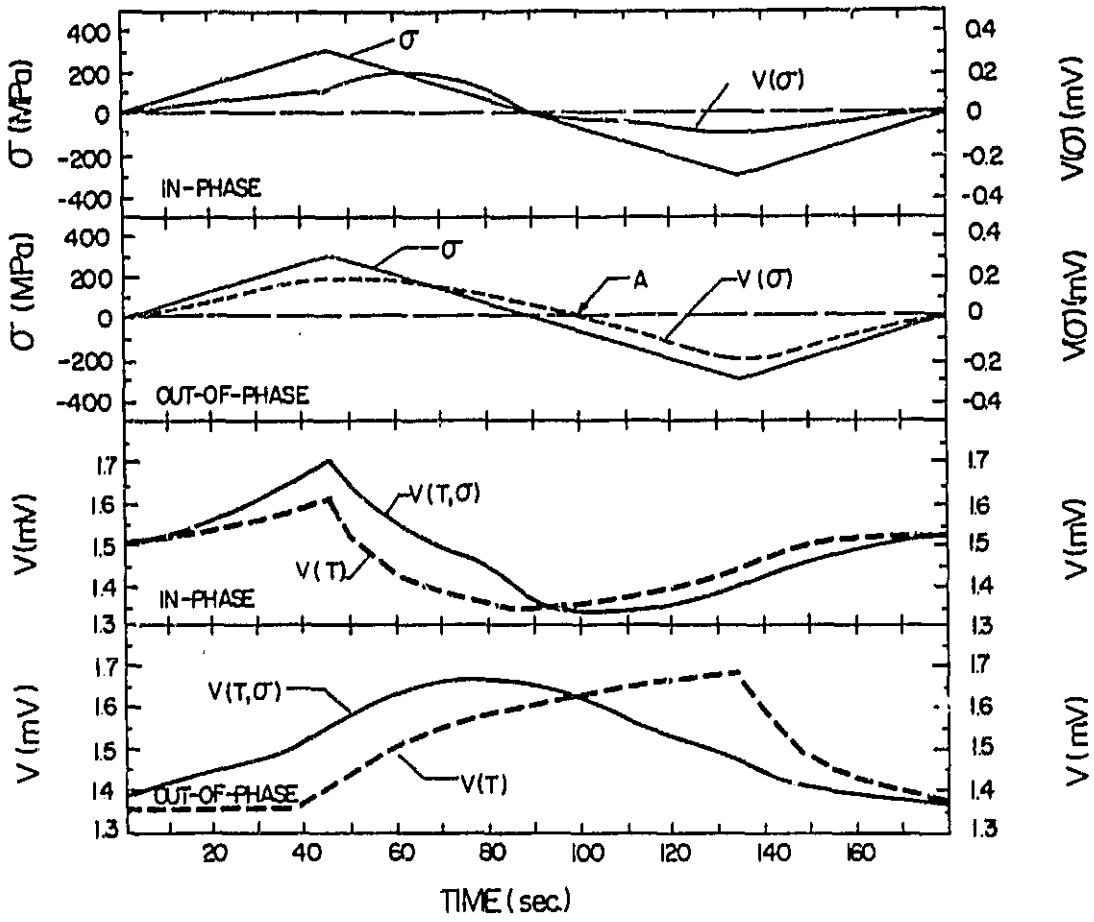

Figure 3 Potential curves $V(T,\sigma)$, $V(T)$ and $V(\sigma)$ for TMFCG of Inconel X-750. ΔK = 50 MPa $\sqrt{m}$.

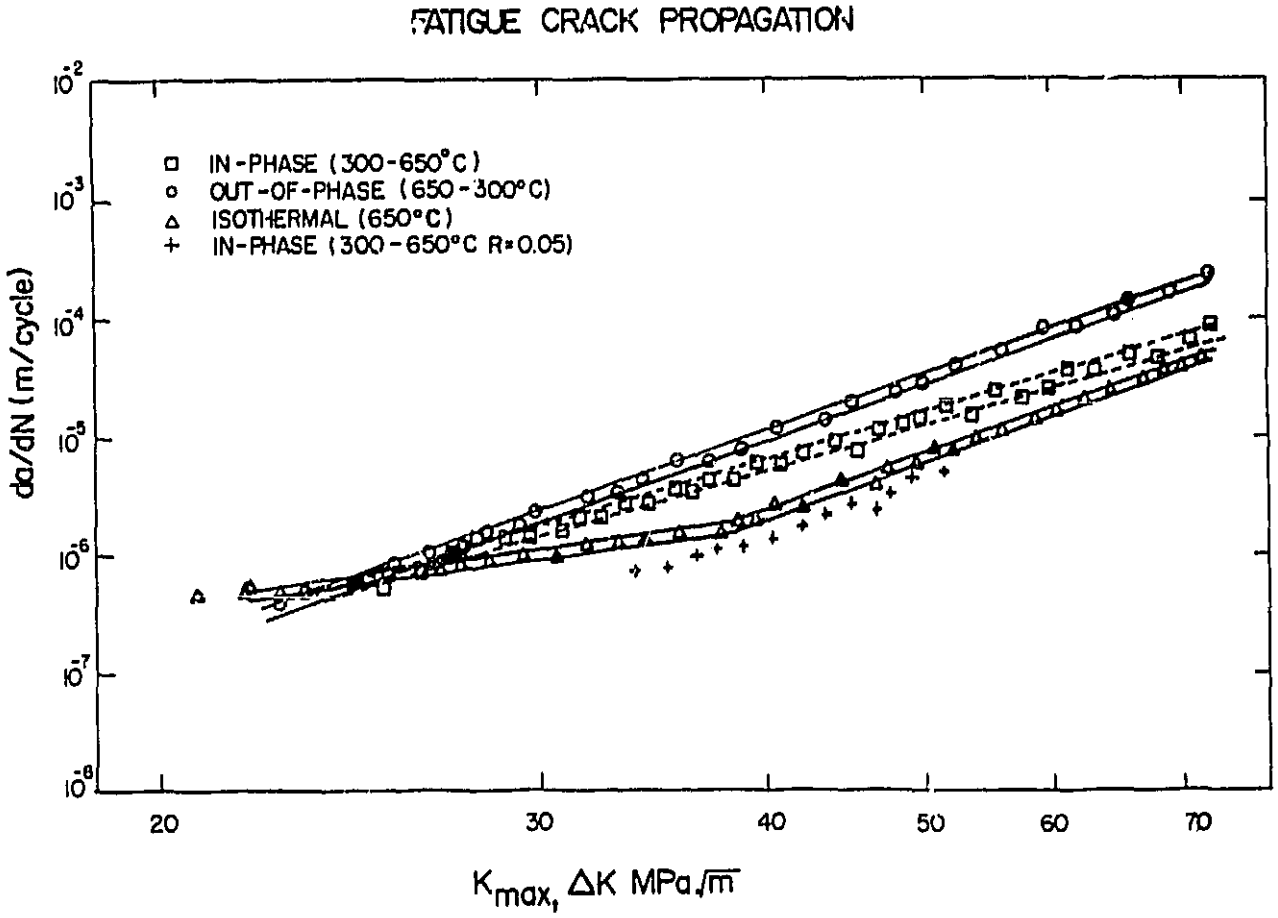

Figure 4 TMFCG of Inconel X-750 as a function of ΔK.

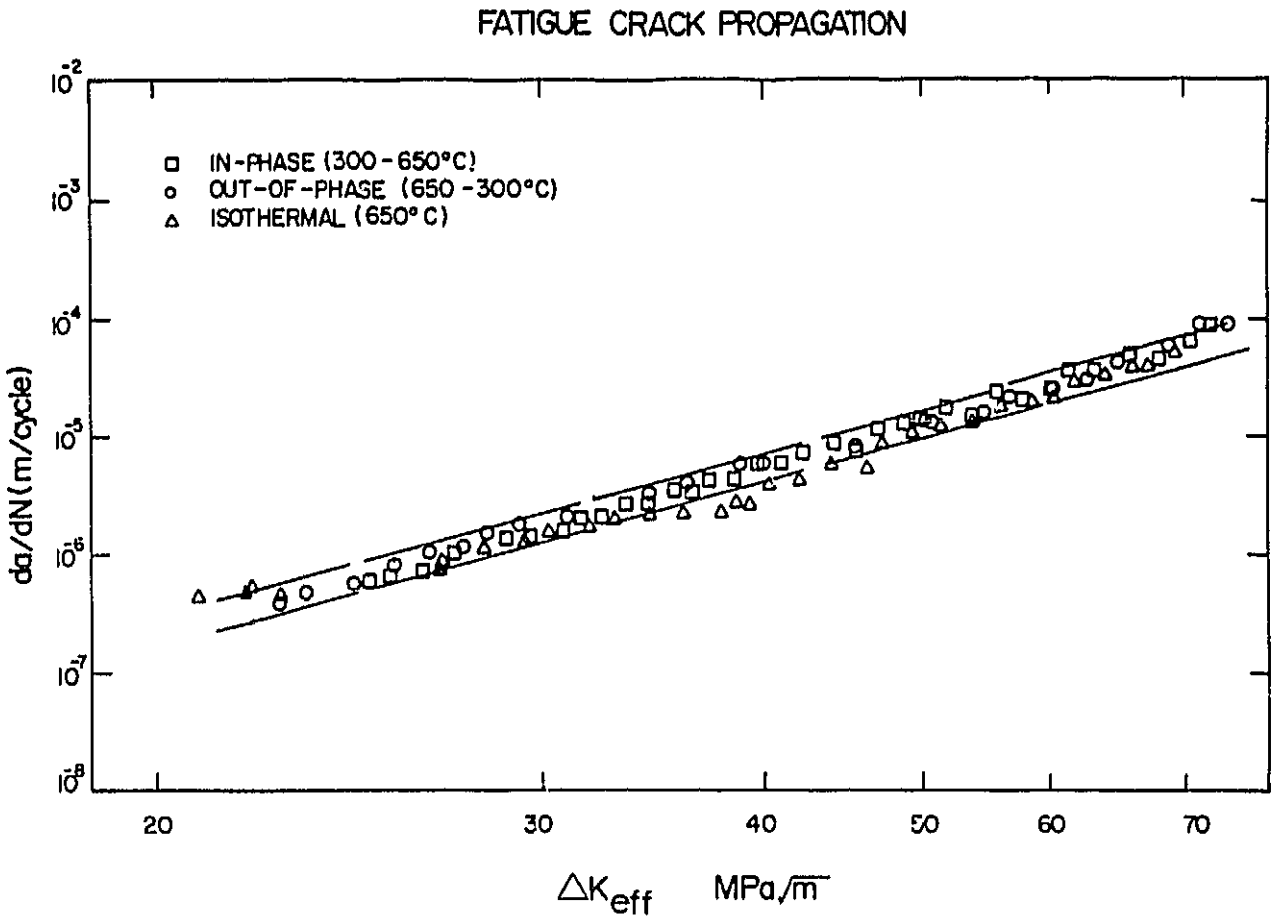

Figure 5 TMFCG of Inconel X-750 as a function of ΔK_{eff}.